Long-term effectiveness of sediment dredging on controlling the contamination of arsenic, selenium, and antimony ☆

Qin Sun [a], Shiming Ding [b, *], Musong Chen [b], Shuaishuai Gao [b, c], Guanghua Lu [a], Yuexia Wu [b], Mengdan Gong [d], Dan Wang [e], Yan Wang [b, f]

[a] Key Laboratory of Integrated Regulation and Resource Development on Shallow Lakes, Ministry of Education, College of Environment, Hohai University, Nanjing, 210098, China
[b] State Key Laboratory of Lake Science and Environment, Nanjing Institute of Geography and Limnology, Chinese Academy of Sciences, Nanjing 210008, China
[c] University of Chinese Academy of Sciences, Beijing, 100049, China
[d] Shanghai Water Source Construction Development Co., Ltd., Shanghai, 200437, China
[e] Shanghai Waterway Engineering Design and Consulting Co., Ltd., Shanghai, 200120, China
[f] Nanjing Easy Sensor Environmental Technology Co., Ltd, Nanjing, 210018, China

ARTICLE INFO

ABSTRACT

This study assessed the effectiveness of dredging in controlling arsenic (As), selenium (Se), and antimony (Sb) contamination in sediments, by examining contaminant concentrations in sediments six years after dredging was completed. High-resolution diffusive gradients in thin films (DGT) and dialysis (HR-Peeper) techniques were used to monitor the concentrations of DGT-labile metalloids and soluble metalloids in sediments, respectively. Results revealed that dredging effectively remediated metalloid contamination in sediments only in April, July and/or January. Compared to non-dredged sediments, the concentrations of soluble and DGT-labile As, Se, and Sb in dredged sediments decreased on average by 42%, 52%, and 43% (soluble), and 54%, 50%, and 53% (DGT), respectively. The effectiveness of the dredging was primarily due to the transformation of metalloids from labile to inert fractions, which increased the ability of the sediments to retain the metalloids, and the slowed rate of resupplied metalloids from available solid pools. In contrast, negligible/negative effects of dredging were seen in October, and the concentrations of soluble and DGT-labile metalloids even increased in some profiles of dredged sediments. This was mainly caused by a release of the metalloids from algal degradation, which may offset the dredging effectiveness.

© 2018 Elsevier Ltd. All rights reserved.

1. Introduction

Arsenic (As), selenium (Se), and antimony (Sb) are metalloids. Selenium is an essential biotic element, but it can have negative or toxic effects on biota when it is present in high concentrations in environmental matrixes (Hamilton, 2004). Arsenic is known to be a highly toxic pollutant, which is garnering significant attention because of its characteristic properties and wide distribution in the environment (Sharma and Sohn, 2009). Over 60 million people are at long-term risk of being exposed to high-levels of As ($>50 \, \mu g/L$), primarily through consumption of contaminated drinking water (McCarty et al., 2011). Antimony has similar toxic properties to As. Concentrations of Sb in mining and smelting areas range from 100 to 4489 mg/kg, potentially posing a risk to humans (Filella et al., 2002; Nakamaru and Altansuvd, 2014). Antimony can be produced by a fission of ^{235}U. The Sb pollution in nuclear waste is also brought into focus (Jan, 2007). As, Sb and Se are defined as precedence pollutants by US-EPA (http://water.epa.gov), and As compounds and Cr(VI) are listed as group 1 carcinogens by the International Agency for Research on Cancer (IARC) (http://www.iarc.fr/).

Lakes are important sources of global freshwater. However, the pollution of waterbodies with metals and metalloids has become an increasing problem in recent years due to increases in industrial, agricultural and other anthropogenic activities (Harikumar et al., 2009). Sediments have been identified as both a sink and source

---

for metal(loid)s pollution in overlying waters (Ni et al., 2016). Dredging is recognized as one of the few methods available for remediation of contaminated sediments (Gustavson et al., 2008) and is frequently used worldwide (Ammami et al., 2015; Fathollahzadeh et al., 2015; Liu et al., 2016). Indeed, dredging has been reported to successfully control nutrient (N, P) and heavy metal (Cd, Hg, Cr, Pb and Cu) pollution in lakes in many previous studies (Guerra et al., 2009; Lin et al., 2011; Mao et al., 2014; Yu et al., 2017; Chen et al., 2018). However, unsuccessful cases involving dredging of contaminated sediments have also been reported (Jiang et al., 2010; Smal et al., 2015). Similarly, dredging has been shown to have two difference effects on As pollution in lakes. Mao et al. (2014) pointed out that sediment dredging was a useful way to reduce the As pollution risk in lake sediments and Wang and Feng (2007) reported that the total As levels in sediments were reduced by 82.6% after dredging. This reduction of total As concentration in sediments may also lead to a decrease of As release from sediments to the overlying water. Wang et al. (2014) reported that the release of As from lake sediments in both wet and dry seasons were reduced by 14.6% and 28.1%, after sediments were dredged. However, Liu et al. (2016) suggested that during dredging, there is a higher risk for As to be released from re-suspended sediments, as they found that dredging resulted in a 31.4% increase in release of As from sediments. Currently, assessments concerning dredging effectiveness for the Se and Sb pollution in lakes are scarce. Therefore, the effectiveness of dredging for removal of metalloid (As, Se and Sb) pollution in lakes is still unclear. It is thus need to play further evaluation in the field.

Most sediment evaluations are based on the changes of total metal/metalloid content and chemical speciation through sequential fractionation (Wang and Feng, 2007; Jiang et al., 2012; Mao et al., 2014). However, these methods are not sensitive enough to reflect dredging effectiveness (Chen et al., 2018), as it difficult to directly evaluate the amount of metalloid pollution in the overlying water and sediments. Furthermore, the geochemistry cycle of metalloids like As are mainly controlled by Fe and Mn redox (Sharma and Sohn, 2009). Furthermore, ex-situ techniques may cause the significant analytical errors because of the changes in redox condition in sediments from air exposure (Wu and Wang, 2017). So, it is necessary to apply an in-situ technique when measuring As, Se and Sb concentrations in sediments when assessment of the dredging effectiveness. The diffusive gradients in thin films (DGT) and dialysis (HR-Peeper) techniques, have been previously applied in the in-situ measurement of DGT-labile and soluble metalloids in sediments at high vertical resolution (Ding et al., 2016; Chen et al., 2017). These techniques have been used to evaluate the influence of dredging on the release of phosphorus in sediment (Yu et al., 2017; Chen et al., 2018), but they are rarely used to assess the effects of dredging on the mobility of metalloids in sediments.

In the present study, the influence of sediment dredging on controlling metalloid pollution was studied in the eutrophic Lake Taihu across four seasons. The concentrations of DGT-labile and soluble As, Se and Sb were monitored in the non-dredged and dredged sediments using high vertical resolution Zr-oxide DGT and HR-Peeper techniques. The kinetics of the metalloids (i.e. release from sediment) were explained by the DGT Induced Fluxes in Sediments (DIFS) modeling.

2. Materials and methods

2.1. Preparation of the DGT and HR-Peeper probes

HR-Peeper and Zr-oxide DGT probes were supplied by Easy-Sensor Ltd. (www.easysensor.net). They were used to simultaneously monitor soluble and DGT-labile As, Se and Sb in the sediments at a 4 mm vertical resolution, respectively. HR-Peepers were constructed using Perspex plates (20 cm) with 30 equally spaced 200-μL chambers and assembled as described in Ding et al. (2010). The chambers were filled with deionized water and covered with Durapore® PVDF membranes (Millipore, 0.45 μm pore size). Assembled HR-Peepers were submerged in deionized water and deoxygenized with N_2 for >16 h before use. DGT membranes were prepared according to Ding et al. (2016). The DGT probe consisted of a Zr-oxide binding gel and a diffusion layer (diffusion gel plus filter membrane). When assembling the DGT probe, the Zr-oxide binding gel was sequentially covered by an agarose diffusive gel and a Durapore® PVDF filter membrane. After that, the DGT devices were submerged in 0.01 M NaCl before use.

2.2. Study sites and field investigation

Lake Taihu is the third largest freshwater lake in China. The surface area, catchment area and volume of the lake are 2338 km^2, 36,500 km^2 and 4.4 billion m^3, respectively (Qin et al., 2007). The north-western region of the lake is characterized by high turbidity and frequent cyanobacterial blooms from late spring through early autumn (Xu et al., 2015). Meiliang Bay is located in the northern part of Lake Taihu and listed as one of the most eutrophic regions, experiencing *Microcystis spp.* bloom every summer. From 2009 to 2010, dredging engineering were taken in the northern part of Meiliang Bay, and approximately 30 cm depth surface sediments were removed from the lake water (Fan et al., 2004; Chen et al., 2018).

Two monitoring sites were selected in the non-dredged (31°26′18″N, 120°11′12″E) and dredged (31°31′33″N, 120°12′33″E) regions in the southern and northern regions of Meiliang Bay, respectively (Fig. 1). Six sediment cores (9 cm in diameter, 30 cm in length) were gathered from each monitoring site in April, July and October in 2016 and then in January 2017. The depths of sediments cores were adjusted to approximately 20 cm. Gathering cores were transported to the laboratory within 3 h. Three sediment cores from each site were selected, sectioned at 0−1, 2−3 and 9−10 cm, and freeze dried for the analysis of metalloid (As, Se and Sb) fractions. Another three sediment cores were placed in a tank and incubated as the same temperature as the field for 2−3 days, to use with HR-Peeper and DGT probes. HR-Peeper probes were first inserted into one of the cores and incubated for 24 h, then the DGT probe was inserted into the same core and they were both deployed for a further 24 h.

2.3. Sampling and analysis

HR-Peeper and DGT probes were recycled and then treated as described in Ding et al. (2010, 2016). After the removal and cleaning of the HR-Peepers, pore water samples (about 200 μL) were immediately collected to use in the determination of soluble As, Se and Sb concentrations. For analysis of DGT samples, Zr-oxide binding gels were vertically sliced into 4 mm sections using a cutter made of stacked ceramic blades. Each slice was eluted with 1.6 mL of eluent (0.4 M NaOH and 1.0 M H_2O_2) for 3−5 h at 4 °C. A sequential extraction method was used to quantify the fractions of As in sediments (Wenzel et al., 2001; Gault et al., 2003; Handley et al., 2013). Arsenic in sediments was divided into five fractions: easily exchangeable arsenic (F1), specifically-sorbed arsenic (F2), arsenic associated with amorphous and poorly-crystalline hydrous iron oxides (F3), arsenic associated with well-crystallized hydrous iron oxides (F4) and arsenic associated with sulfides and organics (F5). A modified European Community Bureau of Reference (BCR) sequential extraction procedure was used to obtain Se and Sb
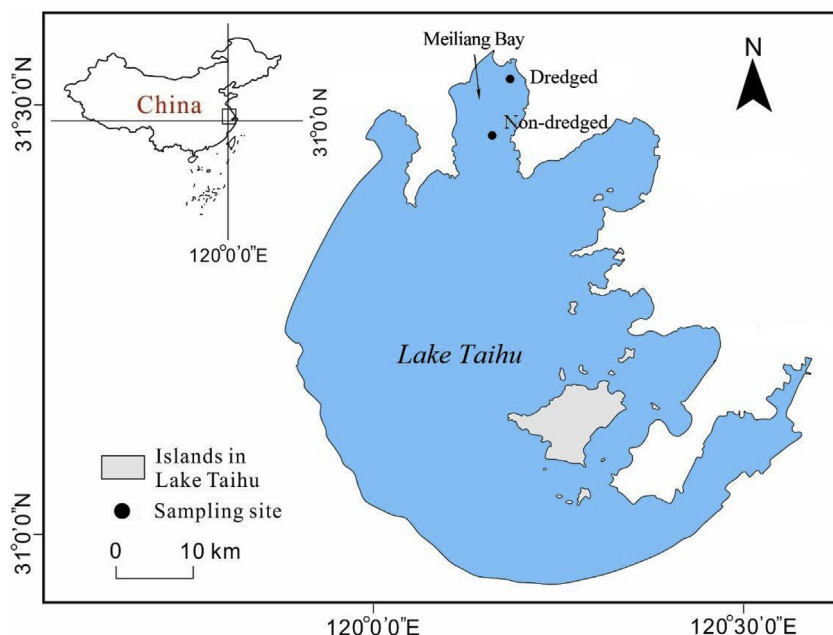
Fig. 1. Location of the sampling site in Meiliang Bay of Lake Taihu.

fractions (Rauret et al., 1999). Selenium and Sb in sediments were divided into four fractions: weak acid extractable, reducible, oxidizable and residual. The concentrations of As, Se and Sb in pore water, 0.4 M NaOH-1.0 M H_2O_2 eluents and in the extracts were analyzed by Inductively Coupled Plasma Mass Spectrometry (NexION 300, Perkin-Elmer).

2.4. Data treatment and statistical analysis

The concentrations of DGT-labile As, Se and Sb in the sediment-water profile were calculated according to equation (1) (Ding et al., 2016):

$$C_{DGT} = \frac{M \Delta g}{DAt} \tag{1}$$

where M represents the accumulated mass over the deployment time; A represents the exposure area of the gel; t represents the deployment time; Δg represents the thickness of the diffusive layer; and D represents the diffusion coefficient of As, Se and Sb in the agarose diffusive layer. D values of those metalloids can be found in a previous study by Wang et al. (2017).

The release kinetics of As, Se and Sb from non-dredged and dredged sediment solids were simulated using the DIFS model (Harper et al., 1998; Harper et al., 2000). The input parameter of R, the ratio of DGT-labile metalloid to soluble metalloid concentration, was calculated as Eq. (2). The distribution coefficient (K_d) for As, Se and Sb were calculated as the ratio of easily exchangeable As, weak acid extractable Se and weak acid extractable Sb to the soluble concentrations of them (Eq. (3)). The output parameter of T_c, which represents the characteristic time for the perturbed system to reach 63% of its equilibrium position, was outputted by the DIFS model. The adsorption (k_1) and desorption (k_{-1}) rate constants were calculated using Eqs. (4) and (5) with T_c and particle concentration (P_c) values.

$$R = \frac{C_{DGT}}{C_{sol}} \tag{2}$$

$$K_d = \frac{C_s}{C_{sol}} \tag{3}$$

$$k_{-1} = \frac{1}{T_c(1 + K_d P_c)} \tag{4}$$

$$k_1 = \frac{k_{-1}}{K_d P_c} \tag{5}$$

Statistical analysis was carried out using SPSS v20.0 software. The differences in metalloid concentration in the sediments (dredged vs. non-dredged) in April, July, October and January were analyzed using independent t-tests, at a $p < 0.05$ level of significance.

3. Results and discussion

3.1. As, Se and Sb in overlying water and surface sediments

The concentrations of soluble As, Se and Sb in the overlying water are shown in Table 1. Their concentrations varied from 4.14 to 24.50 μg/L for As, from 3.60 to 9.05 μg/L for Se, and from 2.41 to 7.12 μg/L for Sb in the non-dredged region. In the dredged region, their ranges were 2.56–16.94 μg/L for As, 1.56–8.98 μg/L for Se, and 1.35–3.15 μg/L for Sb. Compared to the non-dredged region, the concentrations of soluble As were significantly decreased (by 53%) in April in the dredged region. The concentrations of soluble Se also significantly decreased in April and January (by 21% and 60%, respectively). The concentrations of soluble Sb also significantly reduced in April, July and January (by 32%, 44% and 56%, respectively). No significant differences occurred for the concentrations of the three metalloids between in non- and dredged regions in other months. Compared to the permissible limits of the three metalloids in drinking water recommended in China (GB 5749–2006), two concentrations of As and one concentration of Sb exceeded the standards (10 μg/L As and 5 μg/L Sb) in the non-dredged region. In the dredged region, only one concentration of As exceeded the standards. No Se concentrations exceed the (GB 5749–2006)

Table 1
The soluble As, Se, and Sb concentrations in the overlying water and total As, Se, and Sb concentrations in sediments in the non- and dredged sampling sites, respectively.

Parameters		2016—04		2016—07		2016—10		2017—01	
		Non- dredged	Dredged	Non- dredged	Dredged	Non- dredged	Dredged	Non- dredged	Dredged
Overlying water (μg/L)	As	20.22±1.93 [a]	9.56±2.47	24.50±5.94 [a]	16.94±2.61 [a]	4.14±1.63	2.56±0.29	7.68±7.57	7.43±1.86
	Se	9.05±0.81	7.15±1.27	3.60±1.16	1.56±0.64	8.48±1.39	8.98±0.91	6.20±1.10	2.47±0.37
	Sb	4.12±0.61	2.82±0.43	2.41±0.31	1.35±0.05	2.10±0.70	2.47±0.49	7.12±0.87 [a]	3.15±0.96
Surface 10 cm sediments (mg/kg)	Total As	15.35±0.37	28.78±1.44	19.45±0.52	22.94±0.52	14.99±0.37	18.26±0.82	14.55±0.69	12.21±0.21
	Total Se	5.14±0.34	7.69±1.07	5.41±0.38	6.72±0.42	6.61±0.55	6.22±0.54	6.20±0.72	5.51±0.39
	Total Sb	3.04±0.12	6.47±1.21	3.13±0.10	5.55±0.18	3.58±0.05	4.20±0.34	3.58±0.22	3.07±0.21

Underlined data indicates where there was a significant difference ($p < 0.05$) between properties of the overlying water and sediments at non-dredged and dredged sites.
[a] Exceedance of the drinking water quality standards for As (10 μg/L), Se (10 μg/L), and Sb (5 μg/L) set by the Ministry of Health of China (GB5749-2006).

standards in either the non-dredged or dredged regions.

The total concentrations of As, Se and Sb in the 10 cm sediment layer are shown in Table 1. The concentrations of the three metalloids in non-dredged region ranged from 14.55 to 19.45 mg/kg for As, from 5.14 to 6.61 mg/kg for Se, from 3.04 to 3.58 mg/kg for Sb. In contrast, metalloid concentrations in the dredged region ranged from 12.21 to 28.78 mg/kg (As), 5.51—7.69 mg/kg (Se), 3.07—6.47 mg/kg (Sb). There were significantly greater concentrations of As in the dredged region in April (around 187% higher than in the non-dredged region). There were significantly greater concentrations of Se in the dredged region in April and July (around 150% and 124% higher than in the non-dredged region, respectively). There were also significantly greater concentrations of Sb in the dredged regions in April and July (around 213% and 177% higher than in the non-dredged region).

3.2. Chemical speciation of metalloids in sediments

Fractionation of the three metalloids in the sediments are shown in Fig. 2. The As speciation was dominated by F5 in sediments, contributing, on average, 75% and 83% of total As in the non- and dredged regions, respectively. The F5 fraction of As in the dredged region were on average 82% and 83% of total As in the surface 0—1 cm and 3—4 cm layers, which were evidently greater than the 72% and 77% observed in the non-dredged region. Correspondingly, the amount of other As species decreased in the dredged region. As F5 is inert, typically bound to the crystalline lattice of minerals (Mohamed, 2013; Zhu et al., 2015; Chen et al., 2016; Lu et al., 2018), these differences in speciation reflected the transformation of some labile As to inert As in sediments after dredging. A similar phenomenon was observed with Se and Sb speciation. The residual fractions of Se in the surface sediment layers in the non-dredged regions in April, July and October represented an average 28% of total Se, whereas the residual fractions of Se in the dredged region were on average 46% of the total Se. Similarly, the residual fraction of Sb increased from on average 53% of total Sb to 84% of total Sb in the surface sediment layers due to dredging in April and July. Other Se and Sb species, including labile species (exchangeable and reducible fractions), were notably decreased in the dredged regions.

3.3. Changes of soluble and DGT-labile metalloids

The distributions of soluble As, Se and Sb are shown in Fig. 3. For soluble As, there was mostly a trend of increasing concentration with the increase of sediment depth, followed by steady-state or a decrease in concentration on the bottom of the sediment profiles. Only the distribution of soluble As in the dredged region in January showed no evident change with sediment depth. For soluble Se and Sb, their concentrations exhibited no evident increasing or decreasing trends with depth. The mean concentrations of soluble

As, Se, and Sb in each sediment profile are shown in Fig. 5. It is of note that, the concentrations of these metalloids were significantly lower in the dredged region than in the non-dredged region in April, July and January, and their concentrations were 59%, 69% and 46% (for As), 76%, 31% and 38% (for Se), and 47%, 52% and 73% (for Sb) of those in the non-dredged region. In October, there were no significant differences in soluble concentration for the three metalloids.

The distributions of DGT-labile As, Se and Sb are shown in Fig. 4. The distribution patterns of DGT-labile As, Se and Sb were similar to those of soluble As, Se and Sb, shown in Fig. 3. The DGT-labile As initially increased as sediment depth increased, and then either decreased or reached steady-state at the sediment bottom in April, July and October. Only the distribution in January showed no concentration change with depth. Peak-pattern distributions of DGT-labile and soluble As have been previously observed (Bennett et al., 2012; Sun et al., 2016; Yao et al., 2016). This pattern was attributed to the sensitivity of As mobility to the oxic-anoxic transition that occurs between the surface of the sediment and the deep sediment layers (Du Laing et al., 2009a, b, c). Sun et al. (2016) suggested that the reduction of As(V) and the reductive dissolution of Fe(III) (hydr)oxides increased the mobility of As in the upper sediments, while the fixation of As(III) by secondary Fe(II)-bearing minerals decreased the mobility of As in the deep sediments. The distributions of DGT-labile Se and Sb showed no evident decreasing or increasing trends with the increase of sediment depth, which is generally consistent with previous studies measuring these profiles with DGTs (Ding et al., 2016). This demonstrated that the mobility of Se and Sb is not sensitive to the changes in redox condition in the sediments.

Mean concentrations of DGT-labile As, Se and Sb are shown in Fig. 5. In comparison to the non-dredged region, the concentrations of DGT-labile As and Sb in the dredged region were significantly decreased in April and July, with the values being 70% and 35% (As), and 27% and 24% (Sb) lower. The concentrations of DGT-labile Se were significantly reduced in the dredged region in April, July and January, and the concentrations were 71%, 32% and 48% of those in the non-dredged region.

3.4. Kinetics of metalloid mobilization

The resupply kinetics of As, Se and Sb in non- and dredged sediments were simulated by DIFS model. Input and output parameters are shown in Table 2. Most of the R values for the three metalloids were similar or lower in the dredged sediments than in the non-dredged region. This shows that there is a lower ability of metalloids to be released from sediment solids in the dredged region. The K_d values for As and Se were similar or greater in the dredged region, and the K_d values for Sb were lower in the dredged region. This change reflected the ability of the available solids to retain a solute relative to its soluble concentration in the soil
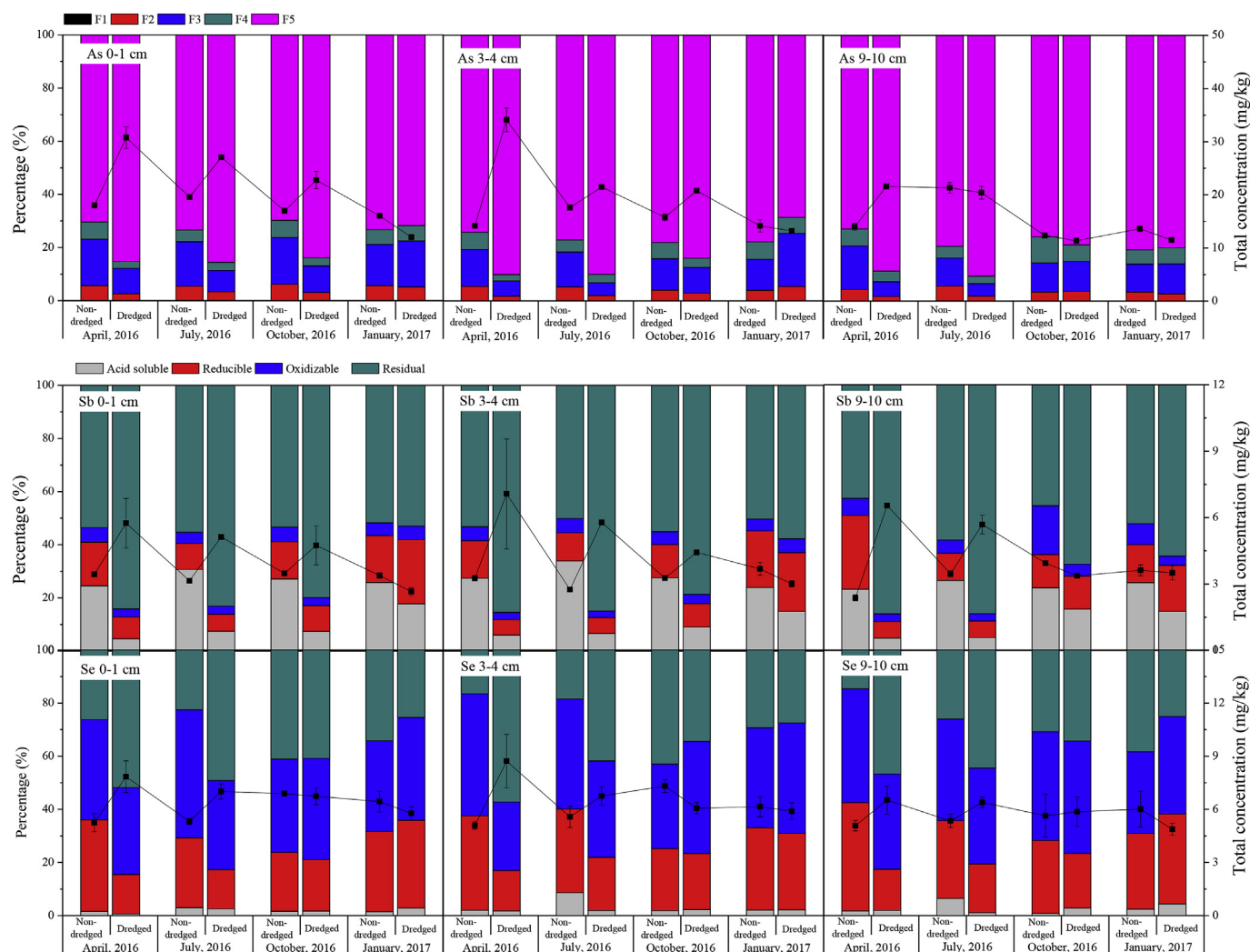
Fig. 2. Seasonal changes of metalloids in total concentrations and their different fractions at depths of 0–1, 3–4, and 9–10 cm in the surface sediments with non- and dredged treatments.

solution under equilibrium conditions (Zhou et al., 2005). Despite the inconsistent changes in K_d, the T_c values of the three metalloids all increased, albeit to different extents, in the dredged region. This increase in T_c value indicated that the sediment required a longer time to reach equilibrium when there was environmental perturbation (Harper et al., 1998). This was further demonstrated by corresponding decreases of k_1 and k_{-1} values in the dredged region.

3.5. Overall assessment of the dredging effectiveness

Until now, assessments of dredging effectiveness have mostly concentrated on nutrients and cationic metals, and reports on oxyanions have been scarce (Chen et al., 2018; Liu et al., 2016; Yu et al., 2017). Furthermore, most of the assessment is based on the changes of total concentrations of the contaminants of interest, and on chemical speciation from sequential fractionation (Wang and Feng, 2007; Jiang et al., 2012; Mao et al., 2014). In this study, we first compared the differences in the concentrations of soluble metalloids in overlying water, and their total contents in surface sediments. The results showed that remediation of sediments via dredging in April, July and then January was effective for the three metalloids, reflected by the decreases in the concentrations of soluble metalloids in the overlying water (Table 1). However, the

total concentrations of the three metalloids in surface sediments significantly increased in April and July (Table 1, Fig. 2), implying that the use of total metalloid contents in sediments can misguide assessment. This further showed the need to use high-resolution passive sampling techniques, which are much more sensitive for demonstrating the mobility of metalloids in sediments (Ding et al., 2016).

Further measurements using HR-Peepers and DGTs revealed a similar change in the concentrations of soluble/DGT-labile metalloids in the overlying water, i.e., both the concentrations of soluble metalloids and DGT-labile metalloids were significantly reduced in April, July and then January in the dredged regions. This highlighted the seasonal fluctuation of dredging effectiveness, with effectiveness decreasing in the following order: spring, summer, winter, and then autumn (where dredging was ineffective). Chemical fractionation showed that labile metalloid fractions transformed into residual fractions in sediments after dredging in April and July (Fig. 2). This implied that the dredged sediment became inert in the two months, which was likely the major reason for the decreasing metalloid mobility, as reflected by the HR-Peeper and DGT measurements (Figs. 3 and 4). The release kinetics of the three metalloids between available solid pools and pore water solutions, simulated using DIFS, supported this hypothesis. Despite the
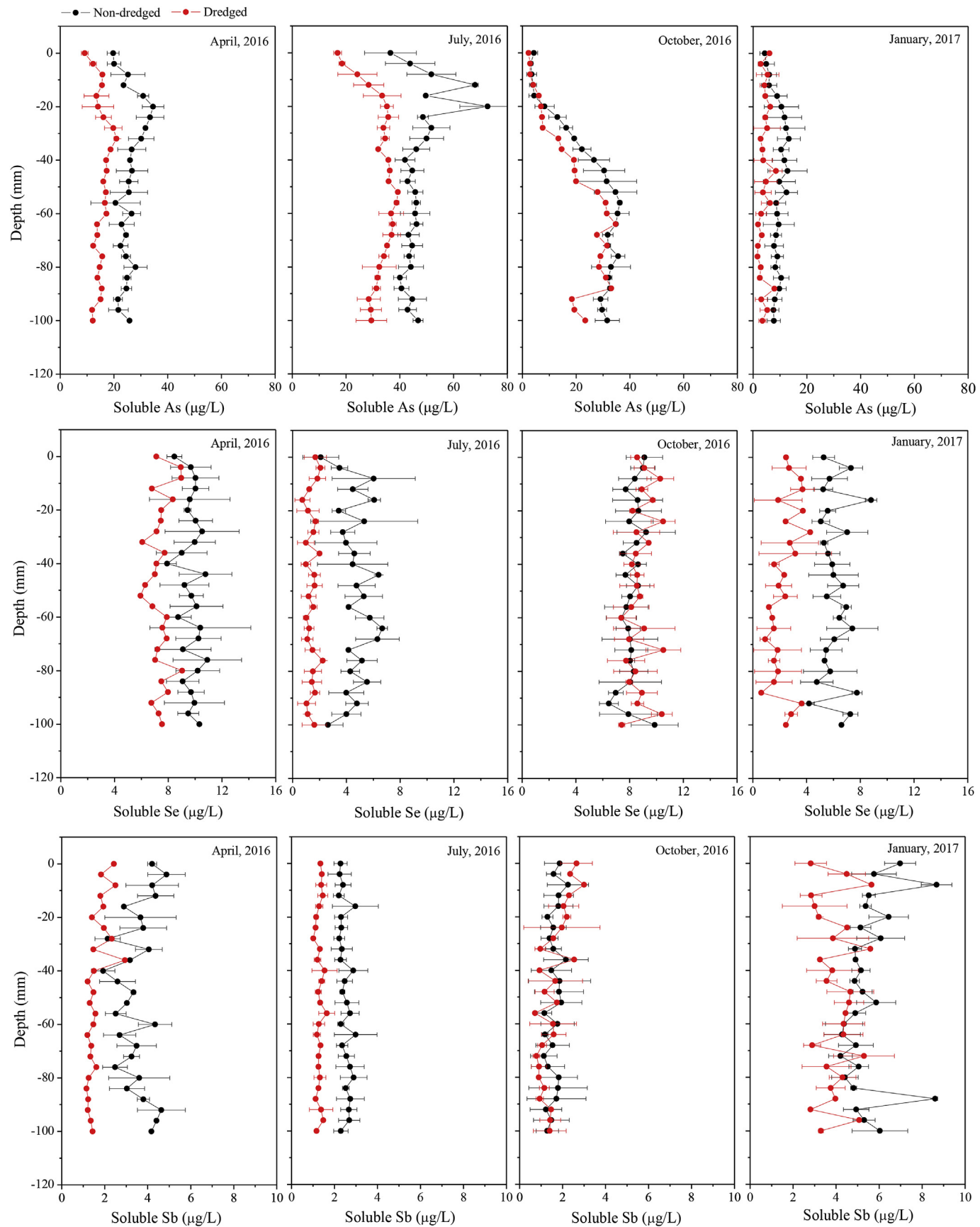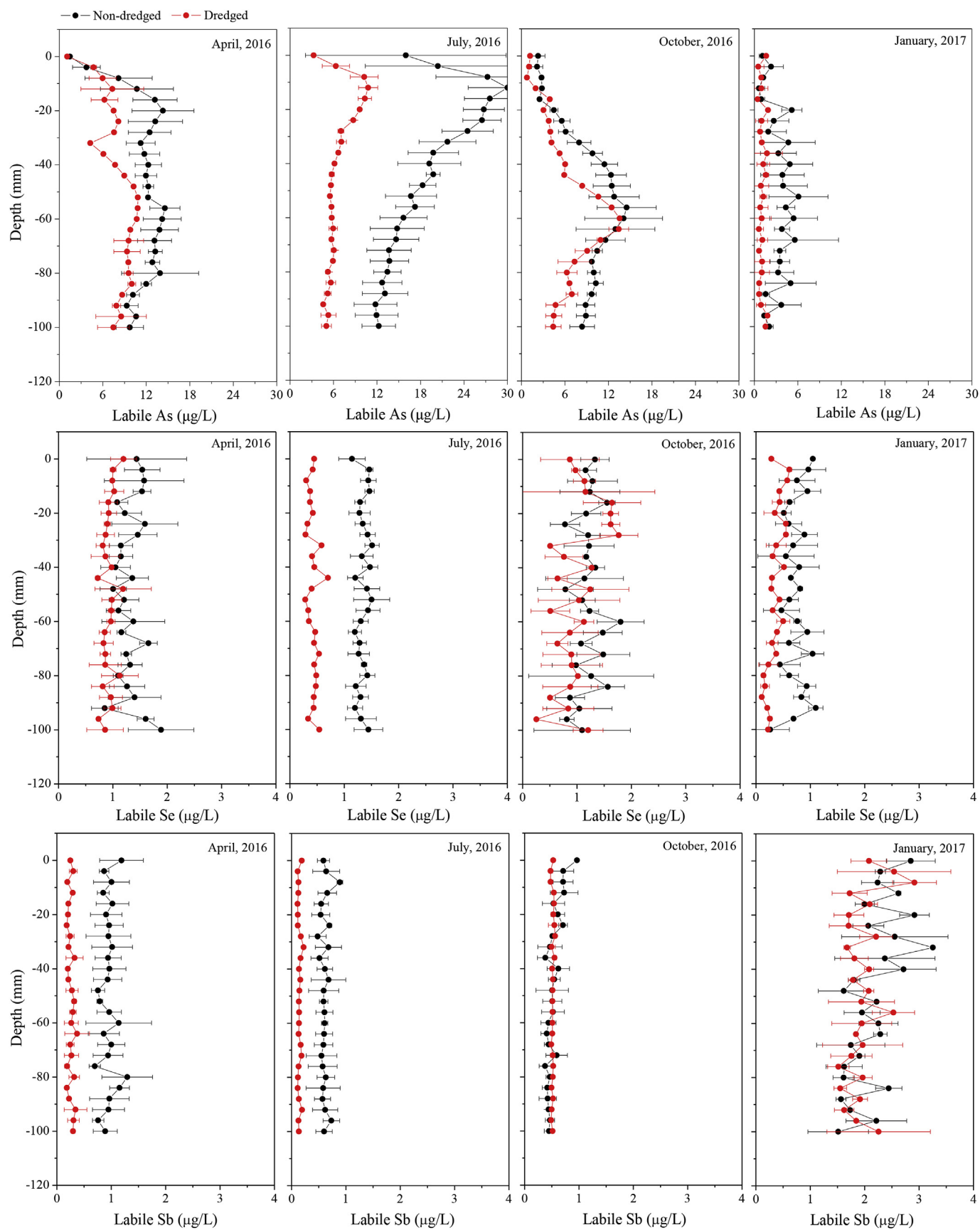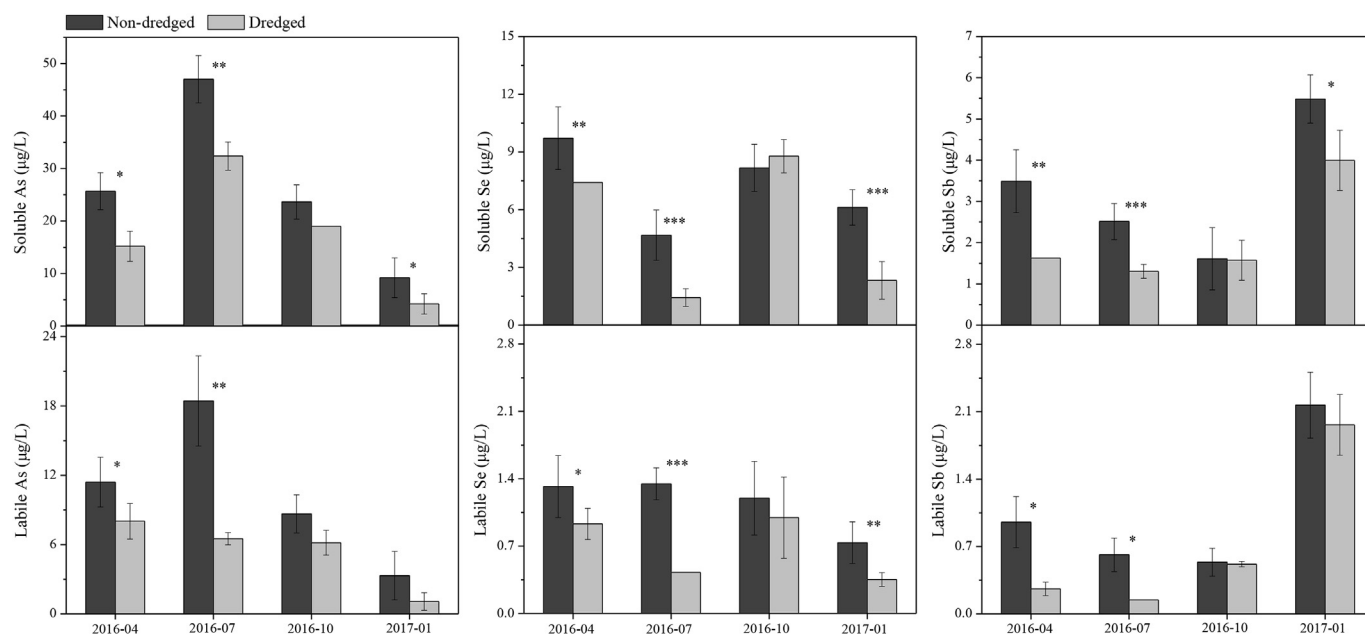
Fig. 3. Seasonal distributions of soluble As, Se, and Sb in pore waters of the non-dredged and dredged sediments, from April 2016 to January 2017.

Fig. 4. Seasonal distributions of DGT-labile As, Se, and Sb in the non-dredged and dredged sediment profiles from April 2016 to January 2017.

Fig. 5. Seasonal changes in mean concentrations of soluble and DGT-labile As, Se, and Sb at a depth of 0 to −100 mm, in non-dredged and dredged sediments from April 2016 to January 2017.

Table 2
Parameters modeled by DGT Induced Fluxes in Sediments (DIFS) for As, Se, and Sb in surface sediments at depths of 0–10 mm in the non-dredged and dredged sampling sites.

	Parameters		2016–04		2016–07		2016–10		2017–01	
			Non-dredged	Dredged	Non-dredged	Dredged	Non-dredged	Dredged	Non-dredged	Dredged
As	Input	R	0.21	0.32	0.48	0.33	0.67	0.37	0.31	0.22
		K_d (cm^3/g)	0.26	0.93	0.39	1.29	1.12	2.81	1.83	1.11
	Output	T_c (S)	4.07×10^{-3}	0.03	0.02	1.48	1.68×10^{-3}	425.2	0.02	0.05
		k_1 (/S)	245.52	33.47	49.70	0.68	594.53	2.35×10^{-3}	62.42	19.50
		k_{-1} (/S)	541.65	20.69	72.60	0.30	306.56	4.83×10^{-4}	19.67	10.11
Se	Input	R	0.16	0.13	0.35	0.21	0.14	0.11	0.15	0.18
		K_d (cm^3/g)	8.73	5.70	40.62	93.20	12.68	12.56	15.54	54.83
	Output	T_c (S)	9.26×10^3	2.26×10^4	0.01	8.93×10^3	2.48×10^4	6.34×10^4	1.38	1.53×10^4
		k_1 (/S)	1.08×10^{-4}	4.42×10^{-5}	73.21	1.12×10^{-4}	4.03×10^{-5}	1.58×10^{-5}	0.72	6.53×10^{-5}
		k_{-1} (/S)	7.12×10^{-6}	4.47×10^{-6}	1.04	6.92×10^{-7}	1.83×10^{-6}	7.23×10^{-7}	0.03	6.86×10^{-7}
Sb	Input	R	0.23	0.11	0.31	0.10	0.42	0.19	0.34	0.58
		K_d (cm^3/g)	191.65	117.33	421.64	278.34	499.86	133.00	123.13	110.19
	Output	T_c (S)	7.40×10^3	7.54×10^4	2.95×10^3	1.23×10^5	9.92×10^2	1.20×10^4	1.78×10^3	0.07
		k_1 (/S)	1.35×10^{-4}	1.33×10^{-5}	3.39×10^{-4}	8.14×10^{-6}	1.01×10^{-3}	8.31×10^{-5}	5.62×10^{-4}	14.40
		k_{-1} (/S)	4.06×10^{-7}	6.51×10^{-8}	4.62×10^{-7}	1.68×10^{-8}	1.16×10^{-6}	3.60×10^{-7}	2.63×10^{-6}	0.08

differences in R and K_d between in non-dredged and dredged regions, the kinetic parameters, T_c, k_1, and k_{-1}, exhibited corresponding responses to the changes in metalloid speciation in the dredged region. Increases in T_c and decreases in k_1 and k_{-1} demonstrated that the desorption and adsorption rates decreased in the dredged sediments, with the sediment requiring a longer time to reach equilibration once the partitioning of metalloids between the available solid and liquid phases was perturbed (Harper et al., 1998). This implied that the release of three metalloids from the available solid pools in the dredged sediments was limited in April and July.

The negligible effect of sediment dredging in October in the sampling site used in this study has also been previously observed by Chen et al. (2018) with phosphorus concentrations. Researchers found that dredging in April, July, and January had pronounced effects on controlling the release of soluble reactive phosphate (SRP), with reductions in SRP diffusion flux of 76.7% in April, 61.3% in July and 86.6% in January. Similar to this study, there were no

significant differences in SRP diffusion flux between non-dredged and dredged sediments in October. The reduction of dredging effect in autumn was attributed to the decomposition of algae during the algal bloom collapse in autumn. As mentioned earlier, the sampling region, Meilang Bay, is dominated by algal blooms from late spring to early winter, and goes through a period of intensive decomposition in autumn (Ding et al., 2018; Xu et al., 2017). It is known that cyanobacteria have high capacity for metalloid bioaccumulation, via absorption onto the cell surface or by assimilation by live or dead algae (Kumar et al., 2015; Prasad et al., 2006). The metalloids accumulated in the algae could then be released during the decomposition of algal residues, leading to an increase of mobile metalloids in sediment-overlying water profiles (Li et al., 2014). A recent study showed that algal degradation from August through October in Meilang Bay caused the concentration of dissolved Zn in overlying water to increase to 338–1023 μg/L, which has exceeded the water quality limit for fisheries in China (100 μg/ L) (Jin et al., 2019). This process could have therefore suppressed

the effectiveness of sediment dredging on controlling the mobility of the three metalloids of interest in October, as observed in this study (Fig. 5). It is of note that, because the enrichment of As, Se and Sb and their chemical speciation in sediments are closely related to the contents of clay and organic carbon, as well as grain size of the particles (Gurung et al., 2007; Shi et al., 2017; Hosseini and Sajjadi, 2018), further studies should be carried out to interpret the dredging effects in combination with these data.

4. Conclusions

This study showed that the effects of dredging over 6 years varied with season in controlling the release of As, Se, and Sb from sediments. In April, July and/or January, dredging successfully reduced the concentrations of soluble and DGT-labile metalloids in sediments and limited their release to the overlying water. Soluble As, Se and Sb concentrations in overlying water decreased on average by 29%, 46% and 44%, respectively, compared to non-dredged regions. The effectiveness of dredging was mainly attributed the transformation of labile metalloid fractions to residual fractions, and was not affected by the larger concentrations of total metalloids in the dredged sediments. Metalloids speciation transformation further inhibited the kinetic release of metalloids from solid pools to pore water. This was reflected by the increase of T_c and decrease of k_1 and k_{-1}. In October, dredging had negligible and negative effects on controlling the release of As, Se, and Sb. This was mainly caused by algal degradation during the autumn months, which suppressed dredging effectiveness by releasing metalloids into the sediment-water interface.

Acknowledgments

Appendix A. Supplementary data

Supplementary data to this article can be found online at https://doi.org/10.1016/j.envpol.2018.11.050.

References

Ammami, M.T., Portet-Koltalo, F., Benamar, A., Duclairoir-Poc, C., Wang, H., Le Derf, F., 2015. Application of biosurfactants and periodic voltage gradient for enhanced electrokinetic remediation of metals and PAHs in dredged marine sediments. Chemosphere 125, 1–8.

Bennett, W.W., Teasdale, P.R., Panther, J.G., Welsh, D.T., Zhao, H., Jolley, D.F., 2012. Investigating arsenic speciation and mobilization in sediments with DGT and DET: a mesocosm evaluation of oxic-anoxic transitions. Environ. Sci. Technol. 46, 3981–3989.

Chen, C.L., Tian, T., Wang, M.K., Wang, G., 2016. Release of Pb in soils washed with various extractants. Geoderma 275, 74–81.

Chen, M., Cui, J., Lin, J., Ding, S., Gong, M., Ren, M., Tsang, D.C.W., 2018. Successful control of internal phosphorus loading after sediment dredging for 6years: a field assessment using high-resolution sampling techniques. Sci. Total Environ. 616–617, 927–936.

Chen, X., Sun, Q., Ding, S.M., Chen, M.S., Fan, X.F., Zhang, L.P., Zhang, C.S., 2017. Mobile arsenic distribution and release kinetics in sediment profiles under varying pH conditions. Water Air Soil Pollut. 228, 1–12.

Ding, S., Chen, M., Gong, M., Fan, X., Qin, B., Xu, H., Gao, S., Jin, Z., Tsang, D.C.W., Zhang, C., 2018. Internal phosphorus loading from sediments causes seasonal nitrogen limitation for harmful algal blooms. Sci. Total Environ. 625, 872–884.

Ding, S., Di, X., Wang, Y., Yan, W., Li, Y., Gong, M., Zhang, C., 2016. Simultaneous measurements of eight oxyanions using high-capacity diffusive gradients in thin films (Zr-oxide DGT) with a high-efficiency elution procedure. Environ. Sci. Technol. 50, 7572–7580.

Ding, S., Sun, Q., Xu, D., 2010. Development of the DET technique for high-resolution determination of soluble reactive phosphate profiles in sediment pore waters. Int. J. Environ. Anal. Chem. 90, 1130–1138.

Du Laing, G., Chapagain, S.K., Dewispelaere, M., Meers, E., Kazama, F., Tack, F.M., Rinklebe, J., Verlooand, M.G., 2009a. Presence and mobility of arsenic in estuarine wetland soils of the Scheldt estuary (Belgium). J. Environ. Monit. 11, 873–881.

Du Laing, G., Meers, E., Dewispelaere, M., Rinklebe, J., Vandecasteele, B., Verloo, M.G., Tack, F.M.G., 2009b. Effect of water table level on metal mobility at different depths in wetland soils of the Scheldt Estuary (Belgium). Water, Air, Soil Pollut. 202, 353–367.

Du Laing, G., Rinklebe, J., Vandecasteele, B., Tack, F.M.G., 2009c. Trace metal behaviour in estuarine and riverine floodplain soils and sediments: a review. Sci. Total Environ. 407, 3972–3985.

Fatollahzadeh, H., Kaczala, F., Bhatnagar, A., Hogland, W., 2015. Significance of environmental dredging on metal mobility from contaminated sediments in the Oskarshamn Harbor, Sweden. Chemosphere 119, 445–451.

Filella, M., Belzile, N., Chen, Y.-W., 2002. Antimony in the environment: a review focused on natural waters: II. Relevant solution chemistry. Earth Sci. Rev. 59, 265–285.

Fan, C.X., Zhang, L., Wang, J.J., Zheng, C.H., Gao, G., Wang, S.M., 2004. Processes and mechanism of effects of sludge dredging on internal source release in lakes. Chin. Sci. Bull. 49, 1853–1859.

Gault, A.G., Polya, D.A., Charnock, J.M., Islam, F.S., Lloyd, J.R., Chatterjee, D., 2003. Preliminary EXAFS studies of solid phase speciation of as in a West Bengali sediment. Mineral. Mag. 67, 1183–1191.

Guerra, R., Pasteris, A., Ponti, M., 2009. Impacts of maintenance channel dredging in a northern Adriatic coastal lagoon. I: effects on sediment properties, contamination and toxicity. Estuar. Coast Shelf Sci. 85, 134–142.

Gurung, J., Ishiga, H., Khadka, M., Shrestha, N., 2007. The geochemical study of fluvio-lacustrine aquifers in the Kathmandu Basin (Nepal) and the implications for the mobilization of arsenic. Environ. Geol. 52 (3), 503–517.

Gustavson, K.E., Burton, G.A., Francingues, N.R., 2008. Evaluating the effectiveness of contaminated-sediment dredging. Environ. Sci. Technol. 42, 5042–5047.

Hamilton, S.J., 2004. Review of selenium toxicity in the aquatic food chain. Sci. Total Environ. 326, 1–31.

Handley, K.M., McBeth, J.M., Charnock, J.M., Vaughan, D.J., Wincott, P.L., Polya, D.A., Lloyd, J.R., 2013. Effect of iron redox transformations on arsenic solid-phase associations in an arsenic-rich, ferruginous hydrothermal sediment. Geochem. Cosmochim. Acta 102, 124–142.

Harikumar, P.S., Nasir, U.P., Rahman, M.P.M., 2009. Distribution of heavy metals in the core sediments of a tropical wetland system. Int. J. Environ. Sci. Technol. 6, 225–232.

Harper, M.P., Davison, W., Tych, W., 2000. DIFS—a modelling and simulation tool for DGT induced trace metal remobilisation in sediments and soils. Environ. Model. Software 15, 55–66.

Harper, M.P., Davison, W., Zhang, H., Tych, W., 1998. Kinetics of metal exchange between solids and solutions in sediments and soils interpreted from DGT measured fluxes. Geochem. Cosmochim. Acta 62, 2757–2770.

Hosseini, M., Sajjadi, N., 2018. The comparison of selenium and lead accumulation between contaminated muddy and sandy sediments from four estuaries along the Persian Gulf: effect of grain size. Environ. Geochem. Health 40 (4), 1645–1656.

Jan, F., 2007. On the removal of silver and antimony radionuclides from radioactive liquid waste by some classical means. Int. J. Nucl. Energy Sci. Technol. 3, 345–357.

Jiang, X., Shi, Z.F., Liu, F., Chen, C.X., Jin, X.C., 2010. Effects of dredging on speciation and bio-toxicity of heavy metals in the surface sediment from Meiliang Bay, Taihu Lake. Res. Environ. Sci. 23, 1151–1157.

Jiang, X., Wang, W., Wang, S., Jin, X., 2012. Calculation of environmental dredging depth of heavy metal polluted sediments in zhushan Bay of Taihu lake. J. Environ. Sci. 33, 1189–1197.

Jin, Z., Ding, S., Sun, Q., Gao, S., Fu, Z., Gong, M., Lin, J., Wang, D., Wang, Y., 2019. High resolution spatiotemporal sampling as a tool for comprehensive assessment of zinc mobility and pollution in sediments of a eutrophic lake. J. Hazard Mater. 364, 182–191.

Kumar, K.S., Dahms, H.U., Eunji, W., Jaeseong, L., Kyunghoon, S., 2015. Microalgae-a promising tool for heavy metal remediation. Ecotoxicol. Environ. Saf. 113, 329–352.

Lin, C.E., Chen, C.T., Kao, C.M., Hong, A., Wu, C.Y., 2011. Development of the sediment and water quality management strategies for the Salt-water River, Taiwan. Mar. Pollut. Bull. 63, 528–534.

Liu, C., Fan, C.X., Shen, Q.S., Shao, S.G., Zhang, L., Zhou, Q.L., 2016. Effects of riverine suspended particulate matter on post-dredging metal re-contamination across the sediment-water interface. Chemosphere 144, 2329–2335.

Lu, H.P., Li, Z.A., Gasco, G., Mendez, A., Shen, Y., Paz-Ferreiro, J., 2018. Use of magnetic biochars for the immobilization of heavy metals in a multi-contaminated soil. Sci. Total Environ. 622, 892–899.

Li, L., Ren, J.L., Yan, C., Liu, S.M., Wu, Y., Zhou, F., Liu, C.G., Zhang, J., 2014. Behavior of arsenic in the coastal area of the Changjiang (Yangtze River) Estuary: influences of water mass mixing, the spring bloom and hypoxia. Continent. Shelf Res. 80, 67–78.

Mao, Z.G., Gu, X.H., Lu, X.M., Zeng, Q.F., Gu, X.K., Li, X.G., 2014. Pollution distribution

and potential ecological risk assessment of heavy metals in sediments from the different eastern dredging regions of Lake Taihu. Environ. Sci.-China 35, 186—193.

McCarty, K.M., Hanh, H.T., Kim, K.-W., 2011. Arsenic geochemistry and human health in south east asia. Rev. Environ. Health 26, 71—78.

Mohamed, I.F., 2013. Environmental geochemistry of el temsah lake sediments, suez canal district, Egypt. Arab. J. Geosci. 6, 4145—4153.

Nakamaru, Y.M., Altansuvd, J., 2014. Speciation and bioavailability of selenium and antimony in non-flooded and wetland soils: a review. Chemosphere 111, 366—371.

Ni, L.X., Li, D.D., Su, L.L., Xu, J.J., Li, S.Y., Ye, X., Geng, H., Wang, P.F., Li, Y., Li, Y.P., Acharya, K., 2016. Effects of algae growth on cadmium remobilization and ecological risk in sediments of Taihu Lake. Chemosphere 151, 37—44.

Prasad, B.B., Banerjee, S., Lakshmi, D., 2006. An AlgaSORB column for the quantitative sorption of arsenic(III) from water samples. Water Qual. Res. J. Can. 41, 190—197.

Qin, B., Xu, P., Wu, Q., Luo, L., Zhang, Y., 2007. Environmental issues of Lake Taihu, China. Hydrobiologia 581, 3—14.

Rauret, G., Lópezsánchez, J.F., Sahuquillo, A., Rubio, R., Davidson, C., Ure, A., Quevauviller, P., 1999. Improvement of the BCR three step sequential extraction procedure prior to the certification of new sediment and soil reference materials. J. Environ. Monit. 1, 57—61.

Sharma, V.K., Sohn, M., 2009. Aquatic arsenic: toxicity, speciation, transformations, and remediation. Environ. Int. 35, 743—759.

Shi, T., Peng, Y., Cao, X., Wang, S., Guo, F., Cao, Y., Liu, J., 2017. Evaluation on distribution and fractionation of antimony in the sediments of yellow river estuary. Fresenius Environ. Bull. 26 (2A), 1528—1537.

Smal, H., Ligeza, S., Wojcikowska-Kapusta, A., Baran, S., Urban, D., Obroslak, R., Pawlowski, A., 2015. Spatial distribution and risk assessment of heavy metals in bottom sediments of two small dam reservoirs (south-east Poland). Arch. Environ. Protect. 41, 67—80.

Sun, Q., Ding, S., Yan, W., Lv, X., Dan, W., Jing, C., Zhang, C., 2016. In-situ characterization and assessment of arsenic mobility in lake sediments. Environ. Pollut. 214, 314—323.

Wang, H., Zhou, Y.Y., Pang, Y., Wang, X.M., 2014. Influence of dredging on sedimentary arsenic release for a tide-influenced waterfront body. J. Environ. Qual. 43, 1585—1592.

Wang, X.Y., Feng, J., 2007. Assessment of the effectiveness of environmental dredging in South Lake, China. Environ. Manag. 40, 314—322.

Wang, Y., Ding, S., Lei, S., Gong, M., Xu, S., Zhang, C., 2017. Simultaneous measurements of cations and anions using diffusive gradients in thin films with a ZrO-Chelex mixed binding layer. Anal. Chim. Acta 972, 1—11.

Wenzel, W.W., Kirchbaumer, N., Prohaska, T., Stingeder, G., Lombi, E., Adriano, D.C., 2001. Arsenic fractionation in soils using an improved sequential extraction procedure. Anal. Chim. Acta 436, 309—323.

Wu, Z., Wang, S., 2017. Release mechanism and kinetic exchange for phosphorus (P) in lake sediment characterized by diffusive gradients in thin films (DGT). J. Hazard Mater. 331, 36—44.

Xu, H., Paerl, H.W., Qin, B., Zhu, G., Hall, N.S., Wu, Y., 2015. Determining critical nutrient thresholds needed to control harmful cyanobacterial blooms in eutrophic Lake Taihu, China. Environ. Sci. Technol. 49, 1051—1059.

Xu, H., Paerl, H.W., Zhu, G., Qin, B., Hall, N.S., Zhu, M., 2017. Long-term nutrient trends and harmful cyanobacterial bloom potential in hypertrophic Lake Taihu, China. Hydrobiologia 787, 229—242.

Yao, Y., Wang, C., Wang, P., Hou, J., Wang, T., Liu, C., Yuan, Y., 2016. In situ, high resolution ZrO-Chelex DGT for the investigation of iron-coupled inactivation of arsenic in sediments by macrozoobenthos bioturbation and hydrodynamic interactions. Sci. Total Environ. 562, 451—462.

Yu, J., Ding, S., Zhong, J., Fan, C., Chen, Q., Yin, H., Zhang, L., Zhang, Y., 2017. Evaluation of simulated dredging to control internal phosphorus release from sediments: focused on phosphorus transfer and resupply across the sediment-water interface. Sci. Total Environ. 592, 662—673.

Zhou, A., Tang, H., Wang, D., 2005. Phosphorus adsorption on natural sediments: modeling and effects of pH and sediment composition. Water Res. 39, 1245—1254.

Zhu, N.M., Luo, T., Guo, X.J., Zhang, H., Deng, Y., 2015. Nutrition potential of biogas residues as organic fertilizer regarding the speciation and leachability of inorganic metal elements. Environ. Technol. 36, 992—1000.